Inriamericwaves
Report of activities - March-May/16

Joao Guilherme Caldas Steinstraesser
José Galaz

May 17, 2016

Contents

1 Introduction

This report presents the initial work developed in the project, between march and may. It was mainly focused on the study and implementation of nonlinear dispersive models for wave propagation: the KdV, the BBM and the Serre equations. In the sections 2 to 4, we describe each one of these models, the theoretical study realized (for example, a scale analysis for the KdV equation) and the proposed discretizations for their computational resolution, using splitting schemes combining finite volume and spectral or finite difference methods. Some examples are presented to illustrate the numerical results and show the problems that must be corrected in the schemes.

Another main subject in which we worked is the study of transparent boundary conditions (TBCs). In the section 5, we describe a first approach to it, with the study of simple approximations to the TBCs in the case of the KdV equation.

2 KdV equation

2.1 The model

The first model of wave propagation studied and implemented in this project is the Korteweg-de Bries (KdV) equation, which takes in account nonlinear and dispersive effects and is a good approximation for waves with small amplitude and long wavelength.

Different forms of this equation can be found in literature, varying mainly in the scaling factors for each physical process present in the equation (nonlinearity and dispersion). We will consider the formulation derived by [1], written in terms of dimensionless but unscaled variables :

$$u_t + u_x + (u^2)_x + u_{xxx} = 0 \tag{1}$$

2.2 Discretization

The problem to be solved, with a initial condition Φ and proper boundary conditions, is

$$\begin{cases} u_t + u_x + (u^2)_x + u_{xxx} = 0 \ , \quad x \in [x_{min}, x_{max}], \quad t \in [0, t_{max}] \\ u(x,0) = \Phi(x) \\ + \text{ boundary conditions} \end{cases} \tag{2}$$

In a first moment, in order to validate the implementation of the model, without influence of the boundaries, we will consider periodic boundary conditions or, in the nonperiodic case, homogeneous Dirichlet and/or Neumann conditions with the boundaries far enough from the propagating wave.

The numerical resolution will be made with a splitting scheme, separating the advective and the dispersive terms. Therefore, defining the operators

$$\begin{aligned} T_a u &= u_t + u_x + (u^2)_x \\ T_d u &= u_t + u_{xxx} \end{aligned} \tag{3}$$

we will solve, in each time step $[t_n, t_{n+1}]$:

$$\begin{cases} T_a(v) = 0 \ \ , \ t \in [t_n, t_{n+1}], \ v(t_n) = u(t_n) \\ T_d(w) = 0 \ \ , \ t \in [t_n, t_{n+1}], \ w(t_n) = v(t_{n+1}) \\ u(t_{n+1}) = w(t_{n+1}) \end{cases} \tag{4}$$

The numerical schemes used in each of these step is descried below :

2.2.1 First step

The first step of the splitted KdV equation is a hyperbolic conservation law, which can be written in terms of a flux function f :

$$v_t + f(v)_x = 0, \quad f(v) = v + v^2 \tag{5}$$

It will be solved using a Finite Volume method, with the cells $[x_{i-1/2}, x_{i+1/2}]$ centered in the discrete spatial points x_i and with the cell-averaged value of the solution equal to the solution in these points (u_i^n). The spatial derivative in (5) will be discretized with a 4th order Runge-Kutta method,

$$\begin{cases} k_1 = -f(v_i^n)_x \\ k_2 = -f\left(v_i^n + k_1 \frac{\Delta t}{2}\right)_x \\ k_3 = -f\left(v_i^n + k_2 \frac{\Delta t}{2}\right)_x \\ k_4 = -f(v_i^n + k_3 \Delta t)_x \\ v_i^{n+1} = v_i^n + \frac{\Delta t}{6}(k_1 + 2k_2 + 2k_3 + k_4) \end{cases} \tag{6}$$

and the spatial derivative will be approximated in terms of the flux on the cells' interfaces :

$$f(v_i^n)_x = \frac{f\left(v_{i+1/2}^n\right) - f\left(v_{i-1/2}^n\right)}{\Delta x} \tag{7}$$

Therefore, we must compute the values of u on each interface. It will be made solving the following Riemann problem :

$$\begin{cases} v_t + f(v)_x = 0 \\ v(x,0) = v^- \ , \ x < 0 \\ v(x,0) = v^+ \ , \ x > 0 \end{cases} \tag{8}$$

where the boundary is located at $x = 0$ and v^- and v^+ are the solutions in its two neighbor cells.

The flux function f is uniformly convex, so the Riemann problem has a unique weak, admissible solution [5] :

- If $v^- > v^+$ (shock) :

$$v(x,t) = \begin{cases} v^- \ , & f(v^-) > f(v^+) \\ v^+ \ , & f(v^-) < f(v^+) \end{cases} \tag{9}$$

- If $v^+ > v^-$ (rarefaction wave) :

$$v(x,t) = \begin{cases} v^- \ , & f'(v^-) > 0 \\ (f')^{-1}(v) \ , & f'(v^-) < 0 < f'(v^+) \\ v^+ \ , & f'(v^+) < 0 \end{cases} \tag{10}$$

2.2.2 Second step

Two schemes will be proposed for the resolution of the second step of the KdV equation,

$$w_t + w_{xxx} = 0 \tag{11}$$

depending on the boundary conditions (periodic or not).

Periodic case The spatial derivatives and the linearity the second step (11) motivates us to implement a Fourier spectral method, which is possible with the periodic boundary conditions. In fact, the method is quite simple :

Let $\hat{w}(k, t_n)$ be the Fourier coefficients of $w(x, t_n)$. The Fourier transform of the equation (11) gives

$$\hat{w})_t(k,t) - ik^3\hat{w}(k,t) = 0 \tag{12}$$

It is an ODE in t, which solution is

$$\hat{w}(k,t) = e^{ik^3(t-t_n)}\hat{w}(k,t_n) \tag{13}$$

Finally, the inverse Fourier transform using the coefficients $\hat{w}(k,t_{n+1})$ gives $w(x,t_{n+1})$

Nonperiodic case For this case, the second equation (11) was solved using an implicit Finite Difference scheme, with fourth order centered discretization of the third spatial derivative, except in the points near the boundaries, for which a simple first order uncentered scheme was used:

$$\begin{aligned}
\frac{u_i^{n+1}-u_i^n}{\Delta t} + \frac{\frac{1}{8}u_{i-3}^{n+1} - u_{i-2}^{n+1} + \frac{13}{8}u_{i-1}^{n+1} - \frac{13}{8}u_{i+1}^{n+1} + u_{i+2}^{n+1} - \frac{1}{8}u_{i+3}^{n+1}}{\Delta x^3} = 0, \quad i = 3, ..., N-3 \\
\frac{u_i^{n+1}-u_i^n}{\Delta t} + \frac{-u_i^{n+1} + 3u_{i+1}^{n+1} - 3u_{i+2}^{n+1} + u_{i+3}^{n+1}}{\Delta x^3} = 0, \quad i = 0, 1, 2 \\
\frac{u_i^{n+1}-u_i^n}{\Delta t} + \frac{u_i^{n+1} - 3u_{i-1}^{n+1} + 3u_{i-2}^{n+1} - u_{i-3}^{n+1}}{\Delta x^3} = 0, \quad i = N-2, N-1, N
\end{aligned} \tag{14}$$

which leads to the resolution of a linear system, with the appropriate modifications to take in account the boundary conditions.

2.2.3 Choice of the time step

The time step is chosen based on the first step of the splitted equation. In the non-conservative form, the equation (5) is written as

$$v_t + (1+2v)v_x = 0 \tag{15}$$

which configures an advection problem with velocity $1+2v$

The space and time steps must verify the CFL condition :

$$(1+2v)\frac{\Delta t}{\Delta x} \leq 1 \tag{16}$$

in order to avoid non-physical behaviors (e.g. mass increasing). Therefore, for each time step, we will chose, for small ϵ

$$\Delta t = \frac{\Delta x}{1 + 2\max\limits_x |v|} - \epsilon \tag{17}$$

2.3 Scale analysis

With the objectif of correctly simulating the physical phenomena involved in the KdV equation, the initial solution must satisfy the assumptions made in the derivation of the model. Following this purpose, we performed a scale analysis following the arguments presented in [1], which at the same time will be linked to the physical case of water surface waves of small amplitude. This analysis will allow us to derive a criteria for selecting the initial conditions of some example simulations.

We will seek to write the KdV equation in the following dimensionless and scaled form, as described in [1]

$$U_T + U_X + \frac{\epsilon}{2}(U^2)_X + \epsilon\alpha^2 U_{XXX} = 0$$

and link it to the parameters involved in the model for surface water waves in dimensional form [4]

$$u^*_{t^*} + c_0 u^*_{x^*} + \frac{3}{4}\frac{c_0}{h_0}(u^{*2})_{x^*} + \frac{1}{6}c_0 h_0^2 u^*_{x^*x^*x^*} = 0 \tag{18}$$

where the $\cdot^*$ denotes the physical variables, h_0 the undisturbed water depth for flat bottom and $c_0 = \sqrt{gh_0}$ the long wave speed.

2.3.1 Characterization of the nonlinearity

According to [1], nonlinearity is characterized by a parameter ϵ such that if characteristics are written in the form

$$\frac{1}{c_0}\frac{dx}{dt} = 1 + bu$$

then one can choose an $\epsilon \ll 1$ such that $bu = \epsilon U$, with U of order one. For the particular case of water waves this can be represented as

$$\frac{1}{c_0}\frac{dx}{dt} = 1 + \frac{3}{2h_0}u$$

and thus $b = \frac{3}{2h_0}$. This parameter will be used in the next arguments.

2.3.2 Characterization of the dispersion

The characterization of the dispersion comes from the derivation of the KdV equation. According to [1] if the propagation of the wave follows a law of the form

$$u^*_{t^*} + uu_x + (\mathcal{L}u^*)_{x^*} = 0$$

with $\mathcal{L}$ such that

$$\hat{\mathcal{L}u^*} = \frac{c(k)}{c_0}\hat{u^*}(k,t)$$

with $\hat{\cdot}$ the Fourier transform and $c(k)$ the phase celerity, which is equivalent to

$$\mathcal{L}u = \mathcal{F}^{-1}\left(\frac{c(k)}{c_0}\right) * u$$

where $\mathcal{F}^{-1}$ is the inverse Fourier transform operator, then new scaling based on the fact that for κ suffiicently small, the wave speed $c(\kappa) = c_0 + c_0\sum_{n=1}^{\infty} A_n\epsilon^n\kappa^{2n}$ can be approximated by $c(\kappa) = c_0(1-\kappa^2)$, which motivates replacing $x = \sqrt{\epsilon}X$, $t = c_0\sqrt{\epsilon}T$, and $u = \frac{\epsilon}{b}U$ to obtain the equivalent equation

$$U_T + \epsilon UU_x + (\mathcal{L}_\epsilon U)_X = 0$$

with $\mathcal{L}_\epsilon$ such that

$$\hat{\mathcal{L}_\epsilon U} = \frac{c(\epsilon^{1/2}K)}{c_0}\hat{U}(K,T)$$

with $K = \sqrt{\epsilon}k$, which after replacing the full series expansion of $c(k)$ leads to

$$\mathcal{L}_\epsilon U = U + \sum_{n=1}^{\infty}(-1)^n A_n\epsilon^n\partial_X^{2n}U \tag{19}$$

and if terms for $n \geq 2$ are neglectable, which is the case for $\epsilon \ll 1$ and if one supposes that all derivatives of U are of the same order of magnitude, then one obtains that

$$\begin{aligned}\mathcal{L}_\epsilon U &= U + A_n\epsilon\frac{\partial^2 U}{\partial x^2}\\ &= U - \alpha^2\epsilon\frac{\partial^2 U}{\partial x^2}\end{aligned}$$

with $\alpha^2 = -A_n$. Replacing in the scaled equation results in

$$U_T + U_X + \frac{\epsilon}{2}(U^2)_X + \epsilon\alpha^2 U_{XXX} = 0$$

Applying the same scaling $x = \sqrt{\epsilon}X$, $t = c_0\sqrt{\epsilon}T$, and $u = \frac{\epsilon}{b}U$ to the physical equation leads to

$$U_T + U_X + \frac{3\epsilon}{4b}(U^2)_X + \frac{h_0^2\epsilon}{6}U_{XXX} = 0$$

from where one concludes that $\alpha^2 = \frac{h_0^2}{6}$

2.4 The criteria

2.4.1 Choice of the wavelength

A sufficient condition for the terms of order greater than 1 in the power series expansion of $\mathcal{L}_\epsilon$ (equation (19)) to be neglectable is that those terms are also neglectable for $c(k)$, given that that all the derivatives of U have an order of magnitude 1

A key point in the derivation of the KdV equation is to assure that the terms for the higher derivatives (for $n > 1$) are small enough to be neglected. Firstly, [1] assumes that all this derivatives have have an order of magnitude 1. Secondly, a sufficient condition for this is that those terms are also neglectable in the series expansion of $c(k)$. Thirdly, also accordingly to [1], the following form is applicable to surface waves :

$$c(\kappa) = c_0\left(\frac{tanh(\kappa h_0)}{\kappa h_0}\right) = c_0\left(1 - \frac{1}{6}(\kappa h_0)^2 + \frac{19}{360}(\kappa h_0)^2 + ...\right)$$

from where we can see that we must choose $\kappa h_0 \ll 1$

Denoting λ as the wavelength, and choosing a constant B such that $\kappa h_0 = B \ll 1$, it follows that $h_0 = \frac{B\lambda}{2\pi}$, and, from the relation $\alpha^2 = \frac{h_0^2}{6}$, we get $\alpha^2 = \frac{B^2\lambda^2}{6(2\pi)^2}$.

2.4.2 Choice of the wave amplitude

From $bu^* = \epsilon U$, with U of unit order magnitude, and since $b = \frac{3}{2h_0}$, the physical variable is written as $u^* = \frac{2}{3}h_0\epsilon U$, $(\epsilon > 0)$, thus if ϵ represents the amplitud of the wave, $\frac{2}{3}\epsilon h_0$ is the wave amplitude (as done in the scale study). Accordingly to [1], the nonlinearity in the KdV equation is valid for $\epsilon \ll 1$. Therefore, ϵ will be chosen taking in account this condition.

2.4.3 Resume

In resume, the proposed criteria to construct the initial data is :

1. Adopt a water depth h_0 (e.g. from the data)
2. Choose a wave amplitude $A = \frac{2}{3}h_0\epsilon$, then the restriction $\epsilon \ll 1$ translates to $\frac{A}{h_0} = \frac{2}{3}\epsilon \ll 1$.
3. Choose a wavelength λ such that $\kappa h_0 = \frac{2\pi}{\lambda}h_0 = B \ll 1$, which translates to $\frac{h_0}{\lambda} = \frac{B}{2\pi} \ll 1$
4. The effect of dispersion over non linearity can be measured by taking the quotient of their coefficients $\frac{\epsilon\alpha^2}{\epsilon} = \alpha^2$.

From another point of view, one can define a wave of amplitude A and wavelength λ and compute the range of depths in which this initial condition is valid, for a given precision :

$$h_0^{valid} = \left[\frac{3A}{2\epsilon}, \frac{B\lambda}{2\pi}\right] \tag{20}$$

This is consistent with the fact that the KdV model is valid for waves with small amplitude and large wavelenght [1].

2.4.4 Examples

We present here some examples to test the proposed numerical solution for the KdV equation. These examples are inspired in those showed in [5]: the initial solutions are gaussian waves (far enough from the boundaries in order to avoid its influence) with different amplitude and wavelength. The idea is to verify the influence of these characteristics on the nonlinear and dispersive effects, and also to check the water depth range in which the propagation of this solution can be modeled by the KdV equation.

The initial solutions used are

1. **Short wave (figure 1a)**
   - $\lambda = 1$
   - $A = 10^{-5}$
   - $h_0^{valid} = [0.15, 0.16]$
2. **Long wave (figure 1b)**
   - $\lambda = 250000$
   - $A = 0.1$
   - $h_0^{valid} = [150, 3979]$

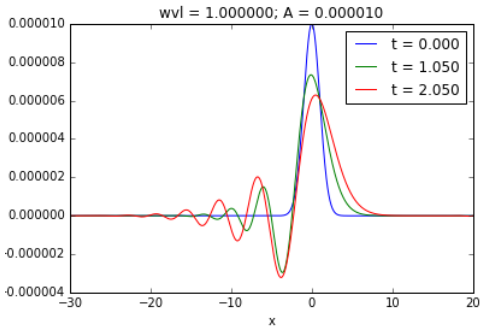

(a) Short gaussian wave

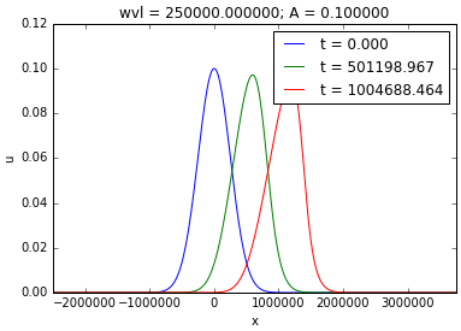

(b) Long gaussian wave

Figure 1: Simulations with the KdV equation

Conclusions :

- These results are compatible with the observations and examples made by [5], which states that dispersive effects are stronger in shorter waves; in the long wave, the nonlinear effect is more evident.
- The range of validity of the KdV equation is very small in the case of the short wave, and much larger for the long wave. This is coherent with the fact that this model is a good approximation for the propagation of long waves with small finite amplitude, which can be seen in the definition of h_0^{valid} (equation (20)) : reducing A and increasing λ increases the length of the interval of validity.
- One of our conclusions in the derivation of the proposed criteria should be revised : the one which says that the importance of the dispersive over the nonlinear effects can be measured by $\alpha^2 = \frac{h_0^2}{6}$: in fact, in the given examples, if we adopt h_0 as the median of h_0^{valid}, the highly-dispersive short wave has a smaller α^2 than the long wave.

3 BBM equation

3.1 The model

The second model for wave propagation that we consider in this project is the BBM equation, which models a long-wave propagation accounting for nonlinear and dispersive effects (in an alternative formulation for the KdV equation, with better stability and numerical properties). This equation is derived by **??** and reads

$$u_t + u_x + (u^2)_x - u_{xxt} = 0 \ , \quad x \in [x_{min}, x_{max}], \quad t \in [0, t_{max}] \tag{21}$$

3.2 Discretization

The BBM model will be treated here in the same way we did for the KdV equation : we will use an split method, leading to the resolution of the following problem in each time step:

$$\begin{cases} v_t + v_x + (v^2)_x = 0 \ \ , \ t \in [t_n, t_{n+1}], \ v(t_n) = u(t_n) \\ w_t - cw_{xxt} = 0 \ \ , \ t \in [t_n, t_{n+1}], \ w(t_n) = v(t_{n+1}) \\ u(t_{n+1}) = v(t_{n+1}) \end{cases} \tag{22}$$

given an initial solution and appropriate boundary conditions.

The first equation (which is exactly the same as in the KdV equation) will be solved with a Finite Volume method, with a 4th order Runge-Kutta discretization for the time derivative, as described in the section 2.2.1. The second equation will be solved with a Fourier spectral method in the periodic case, and a finite difference method in the nonperiodic one, as described below :

Periodic case The second equation of the BBM splitted model can be written as

$$(w - cw_{xx})_t = 0$$

showing that $w - w_{xx}$ does not depend on time. Therefore, for each time step $[t_n, t_{n+1}]$:

$$w - cw_{xx} = (w - cw_{xx})|_{t=t_n} = (v - cv_{xx})|_{t=t_{n+1}} = g(x)$$

This equation will be solved using the Fourier method. Let $\hat{w}(k, t_n)$ and $\hat{g}(k)$ be the Fourier coefficients of $w(x, t_n)$ and $g(x)$ respectively. The Fourier transform of the above equation gives

$$(\hat{w})(k, t) = \frac{\hat{g}(k)}{1 + ck^2}$$

The right-hand side of the last equation does not depend on time. Therefore, the inverse Fourier transform using the coefficients $\hat{w}(k, t)$ gives $w(x, t_{n+1})$

Nonperiodic case ...

3.3 Simulations

...

4 Serre equation

4.1 The model

The Serre equations are a model to describe highly nonlinear waves propagating in shallow waters. Considering a horizontal bottom, these equations are written as

$$h_t + (hu)_x = 0 u_t + u u_x + g h_x - \frac{1}{3h}\left(h^3\left(u_{xt} + u u_{xx} - (u_x)^2\right)\right)_x = 0 \quad (23)$$

where $u = u(x,t)$, $h = h(x,t)$ and g are, respectively, the depth-averaged horizontal velocity of the fluid, the water depth and the gravity acceleration. This formulation is based on [3].

4.2 Discretization

As done previously for the numerical resolution of the KdV and the BBM equations, the Serre equations will be numerically solved using a splitting method, in which the system of equations will be decomposed in two : the first one will contain the advection terms, and the second one, all the high-order derivative terms.

Therefore, the numerical resolution will consist in solve, in each time step $[t_n, t_{n+1}]$, the following problem :

$$\begin{cases} \tilde{h}_t + \left(\tilde{h}\tilde{u}\right)_x = 0 \\ \tilde{u}_t + \tilde{u}\tilde{u}_x + g\tilde{h}_x = 0, \;\; t \in [t_n, t_{n+1}], \quad (\tilde{h}, \tilde{u})(x, t_n) = (h, u)(x, t_n) \end{cases} \quad (24)$$

$$\begin{cases} \overline{h}_t = 0 \\ \overline{u}_t - \frac{1}{3\overline{h}}\left(\overline{h}^3\left(\overline{u}_{xt} + \overline{u}\overline{u}_{xx} - (\overline{u}_x)^2\right)\right)_x = 0, \;\; t \in [t_n, t_{n+1}], \quad (\overline{h}, \overline{u})(x, t_n) = (\tilde{h}, \tilde{u})(x, t_{n+1}) \end{cases} \quad (25)$$

$$\Big\{ (h, u)(x, t_{n+1}) = (\overline{h}, \overline{u})(x, t_{n+1}) \quad (26)$$

If we denote the two systems by the operators $T_a^{\Delta t}$ and $T_d^{\Delta t}$, respectively, where the superscript indicates that the operator is performed over a time step Δt, the problem can be written as

$$(h,u)(x,t_{n+1}) = T_d^{\Delta t}\left(T_a^{\Delta t}\left((h,u)(x,t_n)\right)\right) \tag{27}$$

Some variations of the splitting scheme were also implemented. For example, inverting the order of the operators; or the method known as "strang splitting", in which three problems are solved in each time-step :

$$(h,u)(x,t_{n+1}) = T_a^{\frac{\Delta t}{2}}\left(T_d^{\Delta t}\left(T_a^{\frac{\Delta t}{2}}(h,u)(x,t_n)\right)\right) \tag{28}$$

In the following descriptions of the resolution of the two schemes, the tilde and the overbar will be omitted for the sake of clarity.

4.2.1 First system of equations (advection step)

In order to solve the advection system (24) with the Roe solver (an approximation of the Riemman solver), one must write it in the classical form $U_t + F(U)_x = 0$, where U is the vector of unknowns and F is a flux function. We have that

$$\begin{aligned}(hu)_t = uh_t + hu_t = -u(hu)_x - h\left(uu_x + gh_x\right) = -u\left(h_x u + 2hu_x\right) - ghh_x = \\ -\left(hu^2\right)_x - \frac{1}{2}g\left(h^2\right)_x = -\left(hu^2 + \frac{1}{2}gh^2\right)_x\end{aligned} \tag{29}$$

Therefore, the system can be rewritten as

$$\begin{cases} h_t + (hu)_x = 0 \\ (hu)_t + \left(hu^2 + \frac{1}{2}gh^2\right)_x = 0 \end{cases} \tag{30}$$

and we will solve it for the unknowns $U = \begin{pmatrix} h \\ hu \end{pmatrix}$, with the flux function $F\begin{pmatrix} h \\ hu \end{pmatrix} = \begin{pmatrix} hu \\ hu^2 + \frac{1}{2}gh^2 \end{pmatrix}$. The time step is discretized using a 4th order Runge-Kutta scheme. The Riemman problem in each cell interface will be solved with the Roe solver (an approximated Riemman solver) associated with the MUSCL scheme for the reconstruction of the solution in the interfaces, giving a second order in space.

4.2.2 Second system of equations (dispersive step)

In the second system (25) of the splitted Serre equations , the water depth h is constant in time, and therefore only the velocity u must be updated. Separating the terms containing time derivatives, the second equation of thi suystem can be rewritten as

$$\left(u - hh_x u_x - \frac{1}{3}h^2 u_{xx}\right)_t - \frac{1}{3h}\left(h^3\left(uu_{xx} - (u_x)^2\right)\right)_x = 0 \tag{31}$$

This equation will be solved using an explicit Finite Difference scheme. Defining

$$g_1 = h^3\left(uu_{xx} - (u_x)^2\right)$$

$$g_2 = u - hh_x u_x - \frac{1}{3}h^2 u_{xx}$$

where the derivatives are evalueated using appropriate finite difference approximations.

With this notation, using an one-step forward time discretization, one gets

$$(g_2)_i^{n+1} = (g_2)_i^n + \frac{\Delta t}{3h_i^n}\left((g_1)_x\right)_i^n = G_i^n$$

where the superscript and the subscript denotes respectively the time step and the spatial position.

Using 2nd order centered approximation for the spatial derivatives in $(g_2)_i^{n+1}$, one gets the following tridiagonal linear system :

$$\left(\frac{h_i^n (h_x)_i^n}{2\Delta x} - \frac{(h_i^n)^2}{3\Delta x^2}\right) u_{i-1}^{n+1} + \left(1 + \frac{2(h_i^n)^2}{3\Delta x^2}\right) u_i^{n+1} + \left(-\frac{h_i^n (h_x)_i^n}{2\Delta x} - \frac{(h_i^n)^2}{3\Delta x^2}\right) u_{i+1}^{n+1} = G_i^n$$

with the appropriate modifications to take in account the boundary conditions.

Alternative resolution of the second system (for the variables (h, hu))
Inspired by the discretization described in [2], we will rewrite the second system of equations obtained in the splitting of the Serre equations, in order to solve it in the variables (h, hu) and thus keep the formulation of the first system.

For this purpose, we will multiply the equation (31) and write the variable u inside the time derivative as $\frac{1}{h}hu$:

$$\left(hu - h^2 h_x \left(\frac{1}{h}hu\right)_x - \frac{1}{3}h^3 \left(\frac{1}{h}hu\right)_{xx}\right)_t - \frac{1}{3}\left(g_1\right)_x = 0 \tag{32}$$

Developing the spatial derivatives in (32), we get

$$\left(1 - h^2 - \frac{h^3}{h_{xx}}\right)(hu) + \left(-hh_x - \frac{2h^3}{3h_x}\right)(hu)_x + \left(-\frac{h^2}{3}\right)(hu)_{xx} - \frac{1}{3}\left(g_1\right)_x = 0 \tag{33}$$

which can be written as

$$\tilde{T}(hu)_t = \frac{1}{3}\left(g_1\right)_x \rightarrow (hu)_t = \tilde{T}^{-1}\left(\frac{1}{3}\left(g_1\right)_x\right) \tag{34}$$

where $\tilde{T} = 1 + hT\frac{1}{h}$
and T is an operator defined by Bonneton et al and given by (in the 1D case)

$$Tw = -\frac{h^2}{3}w_{xx} - hh_x w_x \tag{35}$$

Therefore, for each $i = 1, ...N-1$, the actualization of the solution in time is given by

$$(hu)_i^{n+1} = (hu)_i^n + \Delta t z_i^n \tag{36}$$

where $Z = (z_1, z_2, ..., z_{n+1})^T$ is solution of $\tilde{T}Z = \frac{1}{3}\left(g_1\right)_x$. The left side of this system has the form

$$h\frac{z}{h} - h^2 h_x \left(\frac{z}{h}\right)_x - \frac{1}{3}h^3 \left(\frac{z}{h}\right)_{xx} \tag{37}$$

which is solved in the variable z/h (in order to avoid divisions by spatial derivatives of h, that can be equal to zero), leading to the 2nd order discretization

$$\begin{aligned}\left(\frac{h_i^n (h_x)_i^n}{2\Delta x} - \frac{(h_i^n)^2}{3\Delta x^2}\right)\left(\frac{z}{h}\right)_{i-1}^{n+1} + \left(1 + \frac{2(h_i^n)^2}{3\Delta x^2}\right)\left(\frac{z}{h}\right)_i^{n+1} + \\ \left(-\frac{h_i^n (h_x)_i^n}{2\Delta x} - \frac{(h_i^n)^2}{3\Delta x^2}\right)\left(\frac{z}{h}\right)_{i+1}^{n+1} = \frac{1}{3}\left(\left(g_1\right)_x\right)_i^n\end{aligned} \tag{38}$$

4.3 Simulations

4.3.1 Description of the initial solution

In order to validate the implementation of the Serre equations, we will solve it using as initial solution the analytical solution. According to [3], the Serre equations admit the following family of periodic solutions

$$h(x,t) = a_0 + a_1 dn^2(\kappa(x-ct),k)$$
$$u(x,t) = c\left(1 - \frac{h_0}{h(x,t)}\right)$$

$$\kappa = \frac{\sqrt{3a_1}}{2\sqrt{a_0(a_0+a_1)(a_0+(1-k^2)a_1)}}$$
$$c = \frac{\sqrt{ga_0(a_0+a_1)(a_0+(1-k^2)a_1)}}{h_0}$$

with $k \in (0,1)$, $a_0 > 0$ and $a_1 > 0$, $dn(\cdot,k)$ is a Jacobi elliptic function with elliptic modulus k.

The relation between the wavelength λ and $k \in (0,1)$ is

$$\lambda = \frac{2K(k)}{\kappa}$$

and the mean water depth, h_0 is computed as

$$h_0 = \frac{1}{\lambda}\int_0^{\lambda} h(x,t)dx = a_0 + a_1\frac{E(k)}{K(k)}$$

with $K(k)$ and $E(k)$ are the complete elliptic integrals of the first and second kinds.

The limit for $k \to 0^+$ is constant water level $a_0 + a_1$ at rest. If $k \to 1^-$ it converges to the Rayleigh solitary wave solution. We will also test this last case, in which the solution is described by

$$h(x,t) = a_0 + a_1 sech^2(\kappa(x-ct),k)$$
$$u(x,t) = c\left(1 - \frac{a_0}{h(x,t)}\right)$$

$$\kappa = \frac{\sqrt{3a_1}}{2\sqrt{a_0(a_0+a_1)}}$$
$$c = \sqrt{ga_0(a_0+a_1)}$$

The expressions for the wavelength λ and the mean water depth h_0 are the same as shown for the general case of the cnoidal solution.

4.3.2 Results

With the objective to observe the nonlinear and the dispersive processes in the model, we solved the Serre equation and the Nonlinear Shallow Water Equation (NSWE), which is the first step of the proposed split scheme. The figures 2 and 3 shows the evolution of (h, u) for the cnoidal solution; and the figures 4 and 5 for the solitary solution. In this last case, we also solved the problem with a first order finite volume solver for the resolution of the first step of the Serre equation.

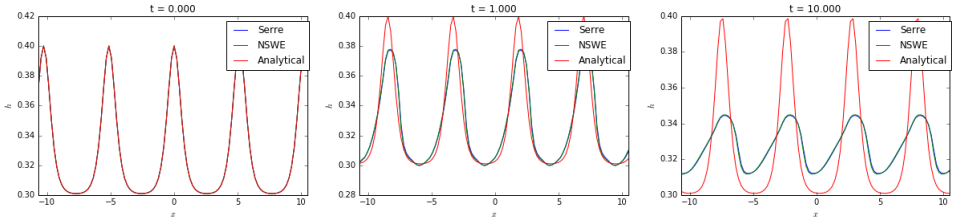

Figure 2: Evolution of h for the cnoidal solution in the Serre equation

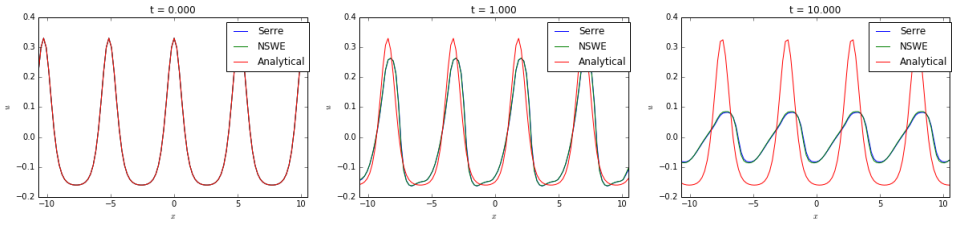

Figure 3: Evolution of u for the cnoidal solution in the Serre equation

The results show the existence of modeling or programming errors. In both cases tested, the analytical solution is not preserved : we observe a strong dissipation of the solution, and, in the solitary wave case, a inversion of the velocity that causes the formation of secondary waves. The utilization of a higher-order solver for the Finite Volume scheme did not corrected this last problem, but showed a lower dissipation.

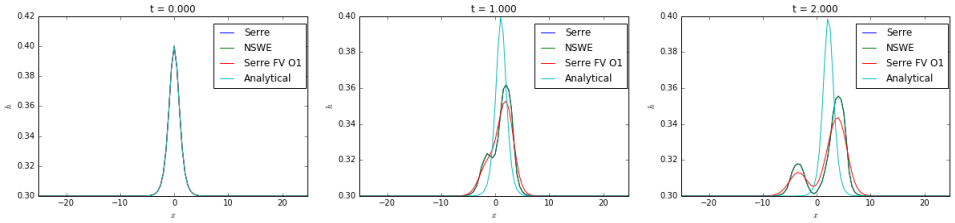

Figure 4: Evolution of h for the solitary solution in the Serre equation

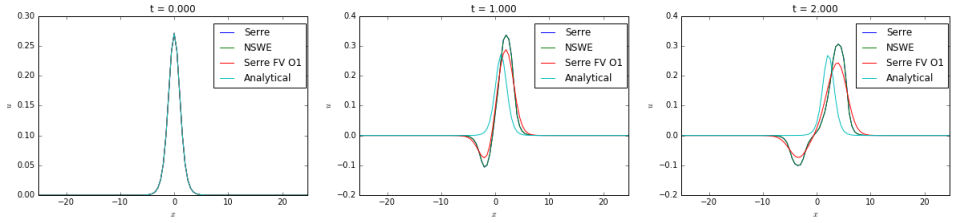

Figure 5: Evolution of u for the solitary solution in the Serre equation

5 Study of transparent boundary conditions

5.1 Introduction and motivational examples

The work presented in this section is an introduction to the objectives that we are looking for in this project, concerning the study of Transparent Boundary Conditions. It was developed on the KdV equation, because, among the models studied and implement until here (Kdv, BBM and Serre equations), it was the one for which we have obtained the best computational implementation.

In the first simulations with the splitting method adopted to the resolution of the KdV equation, we did not make a rigorous application of appropriate boundary conditions. In fact, our initial objective was to validate the method; therefore, imposing periodic or homogeneous Dirichlet and Neumann conditions, we analyzed the evolution of the solution only before the arrival of the wave to the boundaries.

The following example shows very clearly the influence of non appropriate boundary conditions on the solution. We solved two times the same problem, with the same initial solution, boundary conditions, and spatial and time discretizations:

$$\begin{cases} u_t + u_x + (u^2)_x + u_{xxx} = 0 \ , \quad x \in \Omega = [a,b] \quad t \in [0, t_{max}] \\ u(x,0) = \Phi(x) \\ u(a,t) = 0 \\ u(b,t) = 0 \\ u_x(b,t) = 0 \end{cases} \tag{39}$$

The only difference is the size of the domain of each problem : they were chosen such that the wave reaches the boundaries (in the maximal time of simulation) in the first problem, but not in the second. The difference between the solution increases with the time, beginning in the boundary and propagating to the whole domain :

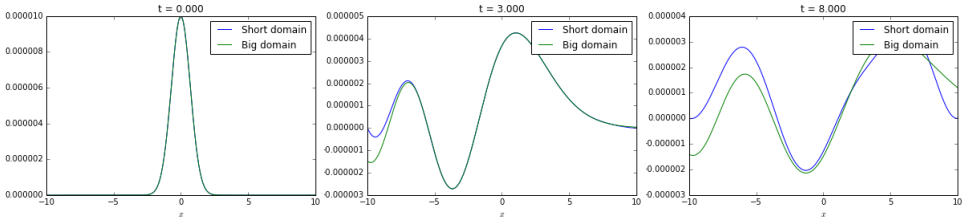

Figure 6: First motivational example : comparison between the solutions in a small and a big domain

Therefore, we look for boundaries conditions that can efficiently simulate the called Transparent Boundary Conditions (TBCs), i.e., in a such a way that the solution calculated in the computational domain Ω coincides with solution of the whole-space restricted to Ω.

In a more practical point of view, we want the boundaries not to have an influence on the solution, so, when the wave reaches the boundary, it will simply "exit" the domain. The following example shows a motivation for this work.

We want to solve the following problem :

$$(P_1) \begin{cases} u_t + u_x + (u^2)_x + u_{xxx} = 0 \ , \quad x \in \Omega_1 = [0, L], \quad t \in [0, t_{max}] \\ u(x,0) = \Phi(x) \\ u(0,t) = 0 \\ u_x(0,t) = 0 \\ u(L,t) = g(t) \end{cases} \tag{40}$$

We seek a function $g(t)$ to simulate the TBC. In order to do this, we will solve before the problem

$$(P_2)\begin{cases} u_t + u_x + (u^2)_x + u_{xxx} = 0\ , \quad x \in \Omega_2 = [0, 2L], \quad t \in [0, t_{max}] \\ u(x,0) = \Phi(x) \\ u(0,t) = 0 \\ u_x(0,t) = 0 \\ u(2L,t) = 0 \end{cases} \tag{41}$$

and we impose $g(t) = u_2(t)$, where u_2 is the solution of (P_2). To obtain more precise results, the two computations are made with the same mesh size and time step.
Suppose that there is a unique solution u_1 to (P_1). We can easily see that $u_2|_{\Omega_1}$ is also a solution of (P_1). Therefore, $u_1 = u_2|_{\Omega_1}$. It justifies why our procedure works as a TBC, as shown in the figure 7 (close-up in the region close to the right boundary) :

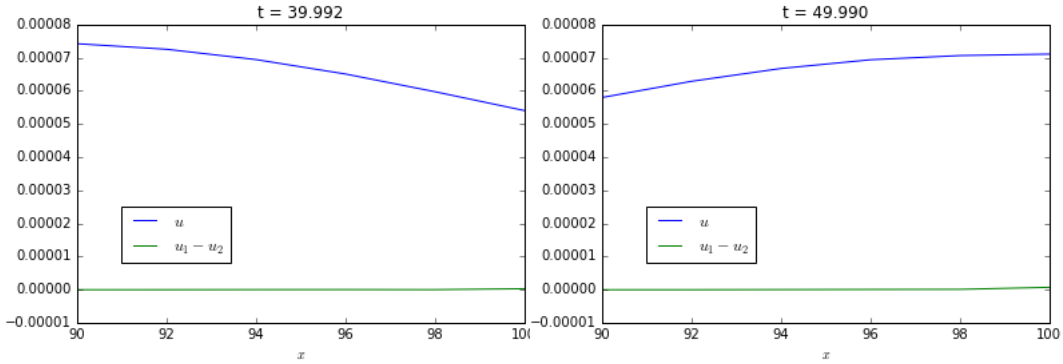

Figure 7: Second motivational example : solution with an "exact" Dirichlet condition at the right boundary

5.2 Robin boundary conditions to simulate TBCs

5.2.1 Robin boundary conditions up to the first derivative

Although the motivating result presented in the above example, we cannot apply this procedure in "real-life" computations. In fact, computing the solution in a larger domain and using it as exact solution is only a trick, which has no practical interest. Therefore, we want to determinate approximations for a TBC without having a referential solution.

The KdV will be solved in the domain $[-L, L]$ with the following boundary conditions (imposed in the resolution of the second equation of the split method):

$$\begin{cases} u(-L) = 0 \\ u_x(-L) = 0 \\ \alpha u(L) + \beta u_x(L) = 0, \quad \alpha, \beta > 0 \end{cases} \tag{42}$$

In the third condition, called a Robin boundary condition, the parameters α and β (or, equivalently, the parameter β/α) will be optimized in order to simulate a TBC. In a first moment, we will consider Robin BCs up to the first derivative of the solution.

To find the optimal coefficients, we will test several pairs $(1, \beta/\alpha)$ (including the limits $\beta/\alpha \to 0$ and $\beta/\alpha \to \infty$, corresponding respectively to Dirichlet and Neumann BCs) and compute the error regarding to a referential solution u_{ref}, computed in a domain $[-2L, 2L]$. Two errors will be computed, for each time step t_n :

$$e_1^n = \sqrt{\sum_{i=0}^{N} (u_i^n - (u_{ref})_i^n)^2} \tag{43}$$

$$e_2^n = u_N^n - (u_{ref})_N^n \tag{44}$$

e_2^n is computed in order to show that most part of the error e_1^n of the entire domain occurs in the boundary.

The figures 8 to 11 show some snapshots and the evolution of e_1 and e_2 for some values of β/α . The figure 12 compares e_2 for many other values, including the pure Dirichlet (with $\alpha = 1, \beta = 0$, so $log(\beta/\alpha) = -\infty$) and pure Neumann (with $\alpha = 0, \beta = 1$, with β/α computationally represented by 10^{10}) conditions.

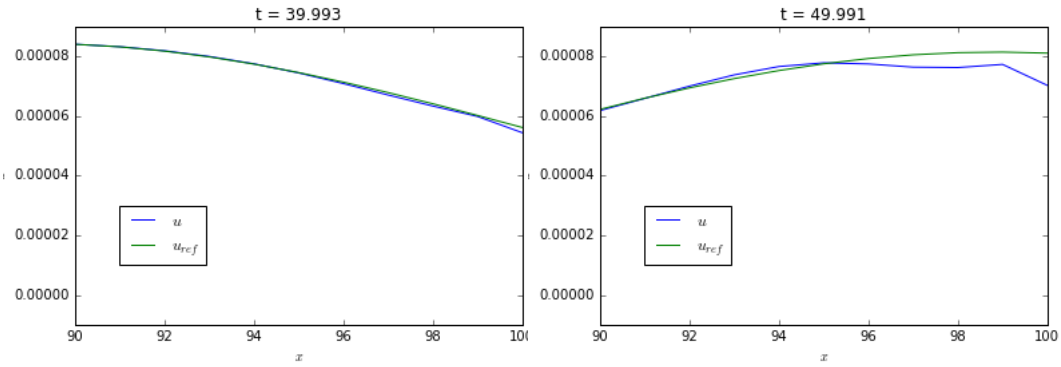

Figure 9: Computed and the referential solution for $\beta/\alpha = 10$

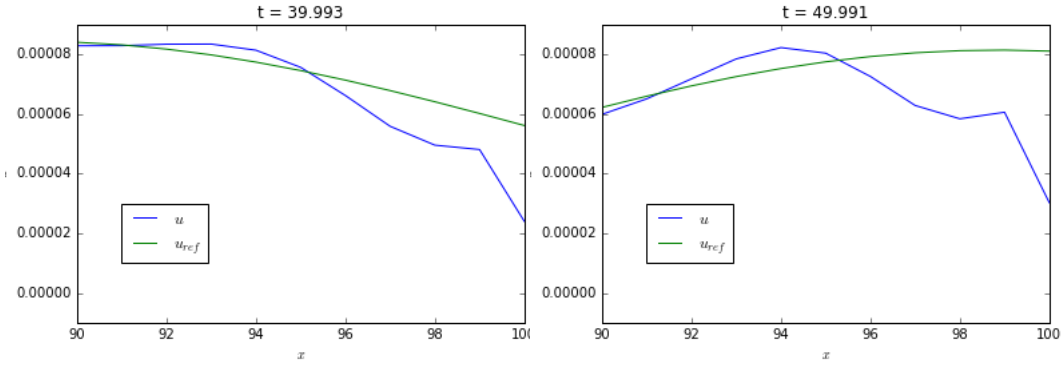

Figure 8: Computed and the referential solution for $\beta/\alpha = 1$

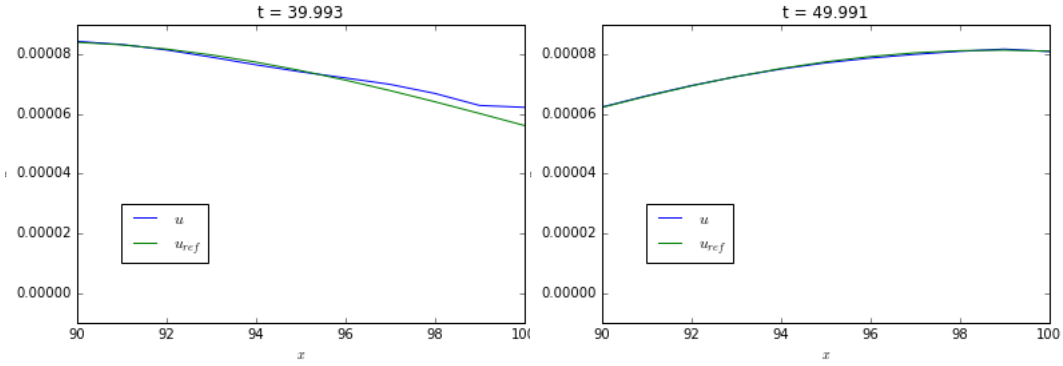

Figure 10: Computed and the referential solution for $\beta/\alpha = 100$

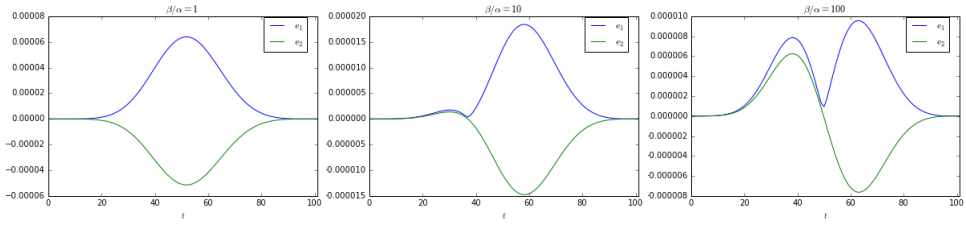

(a) $\beta/\alpha = 1$ (b) $\beta/\alpha = 10$ (c) $\beta/\alpha = 100$

Figure 11: Errors between the computed and the referential solution

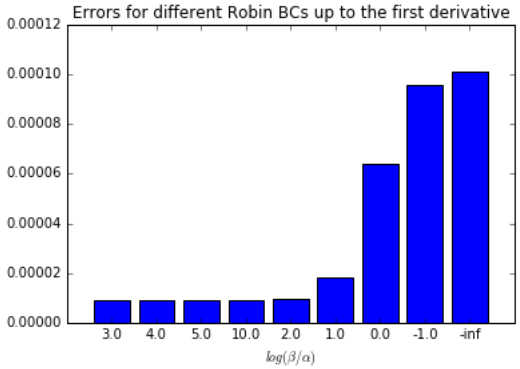

Figure 12: Error e_2 between the computed and the referential solution for many values of β/α

The results presented in the figures 8 to 12 show that boundary conditions with stronger Neumann character produce better approximations to the TBC, compared to more Dirichlet-type conditions. The results for pure Neumann conditions and for Neumann with a small but non-zero Dirichlet were very close.In fact, setting the solution to zero in the boundary is a too much strong condition, and the Neumann condition captures in a more satisfactory way the smoothness of the propagating wave.

5.2.2 Robin boundary conditions up to the second derivative

We repeated the tests described above, but replacing the boundary condition in the right boundary by $\alpha u(L) + \beta u_x(L) + \gamma u_{xx}(L) = 0, \quad \alpha, \beta, \gamma > 0$.

The values of α and β will be fixed and equal to the ones that gave the minimal error in the previous simulations ($(\alpha, \beta) = (1, 1000)$). We will show directly the graph containing the errors for many values of γ/β (figure 13, which should be compared with the figure 12. Similarly to the previous conclusions, we observe a better approximation of the TBCs for stronger values of γ/β.

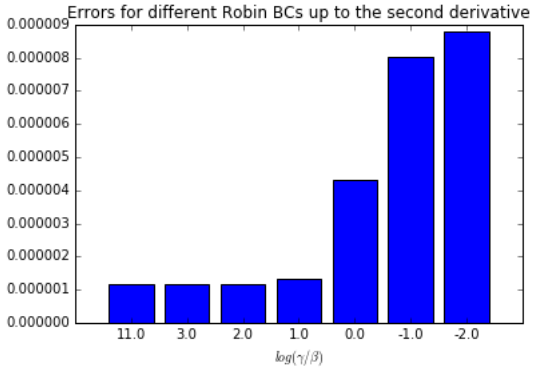

Figure 13: Error e_2 between the computed and the referential solution for many values of γ/β, with Robin conditions up to the second derivative

6 Conclusions and next steps

...

References

[1] T. B. Benjamin, J. L. Bona, and J. J. Mahony. Model equations for long waves in nonlinear dispersive systems. *Philosophical Transactions of the Royal Society of London. Series A, Mathematical and Physical Sciences*, 272(1220):47–78, 1972.

[2] P. Bonneton, F. Chazel, D. Lannes, F. Marche, and M. Tissier. A Splitting approach for the fully nonlinear and weakly dispersive Green-Naghdi model. *J. Comput. Phys.*, 230:1479–1498, 2011.

[3] J. D. Carter and R. Cienfuegos. The kinematics and stability of solitary and cnoidal wave solutions of the Serre equations. *European Journal of Mechanics B/Fluids*, 2011.

[4] Z. Khorsand and H. Kalisch. On the shoaling of solitary waves in the kdv equation. *Coastal Engineering Proceedings*, 1(34):44, 2014.

[5] University of Stanford. Partial differential equations of applied mathematics - lecture 3 : Conservation laws. http://web.stanford.edu/class/math220a/handouts/conservation.pdf, 2002.